Volume 334, number 3, 301–308 FEBS 13260 November 1993

Experimental evidence for 60 Hz magnetic fields operating through the signal transduction cascade

Effects on calcium influx and c-MYC mRNA induction

R.P. Liburdy*, D.E. Callahan, J. Harland, E. Dunham, T.R. Sloma, P. Yaswen

Department of Cell and Molecular Biology, Life Sciences Division, Lawrence Berkeley Laboratory, University of California, Berkeley, CA 94720, USA

Received 12 August 1993; revised version received 29 September 1993

We tested the hypothesis that early alterations in calcium influx induced by an imposed 60 Hz magnetic field are propagated down the signal transduction (ST) cascade to alter c-MYC mRNA induction. To test this we measured both ST parameters in the *same* cells following 60 Hz magnetic field exposures in a specialized annular ring device (220 G (22 mT), 1.7 mV/cm maximal $E_{induced}$, 37°C, 60 min). Ca^{2+} influx is a very early ST marker that precedes the specific induction of mRNA transcripts for the proto-oncogene c-MYC, an immediate early response gene. In three experiments influx of $^{45}Ca^{2+}$ in the absence of mitogen was similar to that in cells treated with suboptimal levels of Con-A (1 μg/ml). However, calcium influx was elevated 1.5-fold when lymphocytes were exposed to Con-A plus magnetic fields; this co-stimulatory effect is consistent with previous reports from our laboratory [FEBS Lett. 301 (1992) 53–59; FEBS Lett. 271 (1990) 157–160; Ann. N.Y. Acad. Sci. 649 (1992) 74–95]. The level of c-MYC mRNA transcript copies in non-activated cells and in suboptimally-activated cells was also similar, which is consistent with the above calcium influx findings. Significantly, lymphocytes exposed to the combination of magnetic fields plus suboptimal Con-A responded with an approximate 3.0-fold increase in band intensity of c-MYC mRNA transcripts. Importantly, transcripts for the housekeeping gene GAPDH were not influenced by mitogen or magnetic fields. We also observed that lymphocytes that failed to exhibit increased calcium influx in response to magnetic fields plus Con-A, also failed to exhibit an increase in total copies of c-MYC mRNA. Thus, calcium influx and c-MYC mRNA expression, which are sequentially linked via the signal transduction cascade in contrast to GAPDH, were both increased by magnetic fields. These findings support the above ST hypothesis and provide experimental evidence for a general biological framework for understanding magnetic field interactions with the cell through signal transduction. In addition, these findings indicate that magnetic fields can act as a co-stimulus at suboptimal levels of mitogen; pronounced physiological changes in lymphocytes such as calcium influx and c-MYC mRNA induction were not triggered by a weak mitogenic signal unless accompanied by a magnetic field. Magnetic fields, thus, have the ability to potentiate or amplify cell signaling.

Signal transduction; Oncogene; c-MYC mRNA; Calcium transport; Extremely-low-frequency (ELF) electric and magnetic field

1. INTRODUCTION

The cell surface is implicated as a major site of interaction for extremely-low-frequency (ELF) electromagnetic fields [1–5]. The parameter associated with the cell surface that is most consistently reported to be influenced by ELF fields, across different laboratories and cellular systems, is calcium transport and binding [1,6–15]. In addition, it is known that calcium plays a critical role in signal transduction (ST) in cells during regulation of growth related processes, e.g. lymphocyte activation and mitogenesis [16,17]. Given this information, an important issue we are addressing in our laboratory is the identification of the biological consequences of a field-induced alteration in calcium ion movement in cells exposed to ELF fields.

The signal transduction cascade is a means of propagating binding events at the cell surface to subsequent 'downstream' events such as RNA and DNA synthesis. The calcium studies mentioned above and calcium's role in ST suggests an interaction site and a general biological framework for understanding ELF field interactions: ELF fields influence events such as DNA and RNA synthesis through alterations in calcium signaling across the cell membrane [1,11,18]. Such a framework provides a mechanism for ELF fields influencing RNA, DNA, and protein synthesis in cells, as has been reported in important studies by Goodman and Henderson [19–21] and Phillips and colleagues [22].

To support the ST hypothesis we present the first measurements of calcium influx and c-MYC mRNA expression in the same cell population of mitogen-activated rat thymocytes exposed to a 60 Hz magnetic field. We observe that mitogen-activated lymphocytes experience a 1.5-fold enhancement of calcium uptake during field exposure and that this is strictly correlated with an approximate 3.0-fold increase in transcript copies for c-MYC mRNA. Transcripts for GAPDH which is a housekeeping gene was not influenced by mitogen or magnetic fields. This data supports the ST hypothesis.

*Corresponding author. Fax: (1) (510) 486 6644.

Specifically the interaction model links alterations in calcium influx across the cell surface to subsequent alterations in DNA, RNA and protein synthesis through the signal transduction cascade. In addition, since the magnetic field acted to trigger signal transduction at suboptimal levels of mitogen it appears that these fields can act as a co-mitogen to amplify cell signaling when weak doses of mitogen are present. Aspects of this study have been presented in abstract form [23].

2. EXPERIMENTAL

2.1. *Cell preparation and calcium transport assay*

Thymic lymphocytes were harvested from Sprague–Dawley rats (250–350 gm) as described [1,7]. Experiments were conducted over an eight month period. In each experiment thymic lymphocytes were harvested from three rats (litter mates), pooled, and employed in studies to simultaneously measure calcium influx and c-MYC mRNA expression in mitogen-activated cells.

Assay buffer was 145 mM NaCl, 1 mM $CaCl_2$, 5 mM KCl, 1 mM Na_2HPO_4, 0.5 mM $MgSO_4$, 5 mM glucose, 10 mM Na-HEPES at pH 7.4, 285 mOsm, 1.685 S/m (37 ± 0.05°C). Cell viability before and after field exposures, determined by Nigrosine dye exclusion, was typically > 97%. Intracellular levels of calcium were assessed after exposures using a rapid, one-step centrifugation assay through a cushion of non-aqueous dibutyl phthalate (DBP) [1,7]; DBP effectively removes aqueous-phase calcium not compartmentalized inside the cell. Assay conditions: thymocytes at 1×10^7/ml, 3 μCi/ml $^{45}Ca^{2+}$, 1 μg/ml of *Concanavalia ensfomis* (Concanavalin A, Con A) (when required), 60 min at 37±0.05°C.

2.2. *Exposure system*

A water-jacketed, solenoidal coil shown in Fig. 1A was fabricated by the Magnet Winding Facility at LBL (400 turns, 2.3 Ω, 20.1 mH) as described [1]. A waterbath assembly was located in the center volume of the solenoid [1,11] into which was placed a specialized glass vessel maintained at 37 ± 0.05°C (Fig. 1B). This specially designed vessel is annular in shape and is analogous to the multiring-annular plate used in previous studies to expose cells to a uniform magnetic field and, at the same time, to a uniform induced electric field which scales as the radius of the annular ring [1,11]. The glass vessel houses up to 50 ml of volume and restricts the location of cells inside of the solenoid to an 'annular ring column' of maximum radius 4.0 cm. By applying Faraday's Law of Induction, the induced electric field experienced by the cells is given by $E_{induced}$ (V/m) = $(r)(f)(\pi)(B_o)$, where r is the annular radius in meters, f is the frequency in Hz, and B_o is the magnetic flux density in Tesla [24,25]. The induced current density experienced by the cells is given by J (A/m^2) = $\sigma_{media} \times E_{induced}$, where σ_{media} was measured to be 1.685 S/m. The sinusoidal 60 Hz magnetic field used in these experiments was 22 mT (220 G) resulting in a maximum induced electric field of 1.7 mV/cm ($radius_{max}$ = 4.0 cm). The current density associated with this induced electric field is given by $J = (\sigma)(E)$, so that J = 0.286 A/m^2 (28.6 μA/cm^2).

Thymocytes in one annular glass vessel were treated with magnetic fields while an identical vessel was simultaneously placed into an isothermal, μ-metal shielded, remote waterbath, which served as the control treatment. The static geomagnetic field parallel to the long axis of the cylindrical annular vessel in the solenoid device and in the control waterbath was < 20.5 μT. The ambient 60 Hz magnetic field parallel to the cylindrical annular vessel in the control waterbath was < 0.1 μT.

2.3. *Northern blot hybridization and quantitation*

Aliquots of cells from the *same* samples used in the calcium influx experiments were assessed for c-MYC and GAPDH mRNA by Northern analyses. RNA was extracted from thymocytes, size fractionated by agarose gel electrophoresis, blotted to nylon membranes and probed for c-MYC and GAPDH mRNA; RNA extractions, hybridizations with ^{32}P-labeled probe, and ethidium bromide staining were performed as described [26]. The c-MYC probe was a gift from Dr J. Campisi of LBL. This probe is a 2.2 kb cDNA clone (pM c-MYC 54) of the mouse c-MYC mRNA [27]. PCR amplified cDNA to the housekeeping enzyme glyceraldehyde-3-phosphate dehydrogenase, GAPDH, was employed as the internal standard for relative amounts of RNA loaded in each lane [28]; transcript levels of GAPDH were similar across sample treatments indicating that general activation of RNA did not occur during suboptimal Con-A treatment and magnetic field exposures (see below). All Northerns were performed in triplicate. Exposures of films were made so that maximum signals detected were within the linear response range. The relative difference in band intensity of c-MYC mRNA transcripts present in the Northerns were quantitated by digital imaging using a cooled-CCD camera, discussed below. This approach provided three independent Northern blot hybridizations for each RNA sample from each treatment group per experiment. Triplicate Northern analysis of each sample permitted a statistical evaluation of results across experiments.

Quantitation of Northerns was performed as follows. Autoradiograms and negatives of UV illuminated ethidium bromide-stained nylon membrane photographs (Polaroid type 55 Pos/Neg film) were imaged in a dark room using a cooled-CCD camera (Photometrics CH220 camera head containing a Thompson TH-7863 frame transfer CCD chip and Uniblitz shutter; CC200 camera controller, CE200 electronics unit containing a 50 kHz, 14 bit A/D card; Photometrics Ltd., Tucson AZ) mounted on a light table (Plannar Technology Model 14 × 17, Gordon Instruments, Inc., Orchard Park, NY). Extraneous illumination was masked off using the table's shutter system and a Nikon 50 mm camera lens (f22, 0.2 s exposure time) was used to acquire images. This system was calibrated by taking images of a calibrated step wedge for optical density (no. T2115, Stouffer Graphic Arts Equipment Co., South Bend, IN) [29]. Images were quantitated as optical density (O.D.) × mm^2 employing a computer program for image calibration and quantitation written using IDL (Interactive Data Language, v.2.3.2, Research Systems, Inc., Boulder, CO). Results obtained using our imaging equipment and software were compared to results from a commercial image analysis system (PDI Imageware Systems, Huntington Station, NY); autoradiograms analyzed on both systems gave similar results. The region of linear response for Kodak X-OMAT, AR film used in these studies was determined from ladder gels of mRNA across a range of loading masses and exposure times. In our system, background-corrected mean O.D. values between 0.03 and 0.60 resulted in linear plots of OD × mm^2 vs. mRNA concentration with a zero y-intercept (corresponding ethidium bromide stained nylons also gave linear plots of O.D. × mm^2 with a zero y intercept). The ratio of 28S to 18S was approximately 2, indicating no significant RNA degradation [29].

2.4. *Statistical analysis*

All data was analyzed for statistical significance across experiments using the multifactor analysis of variance program available in Statgraphics-Plus (Manugistics, Inc., Rockville, MD, USA).

3. RESULTS

3.1. *60 Hz magnetic fields increase calcium ion influx in mitogen-activated thymocytes*

The special annular cylindrical glass vessel shown in Fig. 1B was used to expose cells to a 22 mT magnetic field (maximum $E_{induced}$ = 1.7 mV/cm) or concurrently to an isothermal, μ-metal-shielded control waterbath at 37°C for 60 min. Fig. 2 depicts the results from three independent experiments in which calcium influx was measured in thymic lymphocytes in the absence of Con-A, in the presence of a suboptimal dose of Con-A

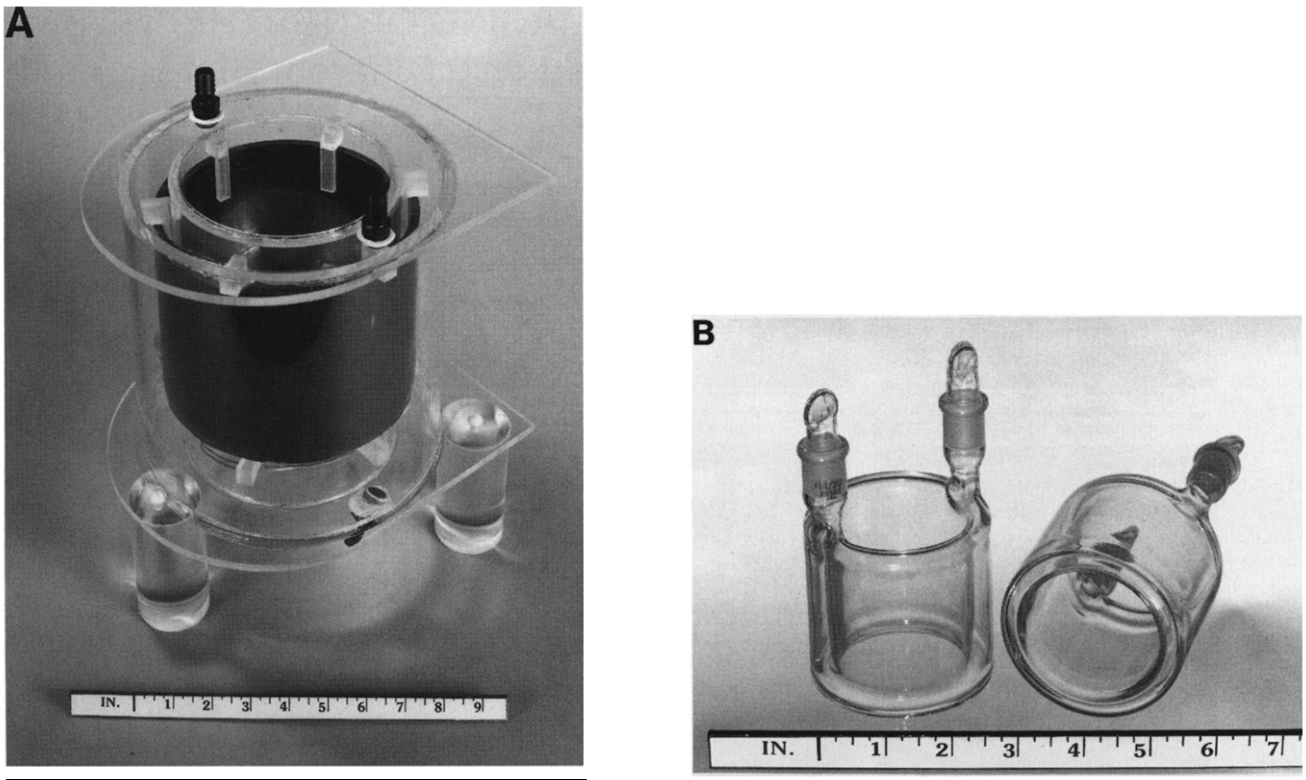

Fig. 1. Solenoid exposure system. (A) A water-cooled solenoid (400 turns, 2.3 Ω, 20.1 mH) was used to establish a 60 Hz magnetic field of 22 mT_{rms} (220 G_{rms}) in the middle-third volume of the solenoid. (B) Cylindrical annular glass vessels used to position the thymocyte cell suspension in an 'annular ring column' with maximum radius of 4.0 cm.

(1μg/ml), and in the presence of suboptimal Con-A plus a magnetic field. Non-activated thymocytes (no Con-A) exhibited a baseline calcium influx of 10,400 ± 386 cpm/10^7cells. A suboptimal dose of Con-A at 1 μg/ml did not result in a significant increase in calcium influx. However, when cells were exposed to a 22 mT magnetic field in the presence of Con-A, a 1.5 fold increase in calcium influx was observed ($P < 0.0001$, F ratio = 48.24). This finding is consistent with previous reports from our laboratory of enhanced calcium influx for mitogen-activated thymocytes exposed to a 22 mT, 60 Hz magnetic field [1,6,11,18]. It is important to note that mitogen-activated calcium influx in lymphocytes is dependent on animal age, mitogen dose, and immune status of the animal [11,18]. In the studies presented here each of the independent experiments employed thymocytes pooled from three, age-matched animals, and this pooled population responded suboptimally to a dose of 1 μg/ml of Con-A. This permitted detection of an increase in calcium influx of Con-A treated cells due to the field. Cells maximally activated by Con-A are at their maximal dynamic limit and further calcium influx in response to an applied magnetic field is not possible.

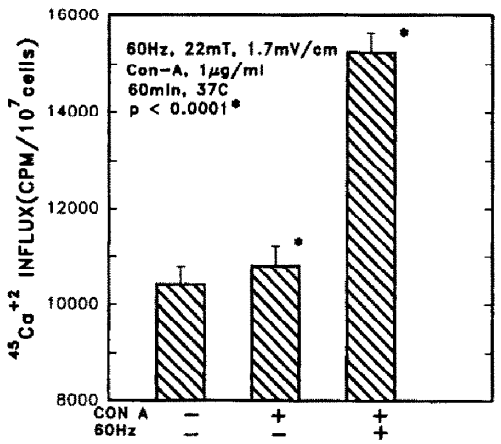

Fig. 2. 60 Hz sinusoidal magnetic fields increase calcium influx in Con-A activated rat thymocytes. Exposures at 22 mT_{rms} (220 G_{rms}), 1.7 mV/cm, 28.6 $\mu A/cm^2$, 37.0 ± 0.05°C, 60 min. Con-A at 1 μg/ml when present. Samples were simultaneously analyzed for GAPDH (Fig. 4) and c-MYC mRNA induction (Fig. 5); mean ± S.E. for data from three independent experiments.

3.2. *60 Hz magnetic fields increase c-MYC mRNA copies in mitogen-activated thymocytes: quantitation by cooled-CCD imaging*

Fig. 3 depicts Northern blot analyses that were repeated three times on the same RNA sample from one experiment to demonstrate the precision and reproducibility of this technique prior to optical density calibration and GAPDH normalization. Panel A shows the images obtained for each Northern. Panel B represents the regions of interest for the three bands in each Northern. Panel C shows the image after flat-fielding and

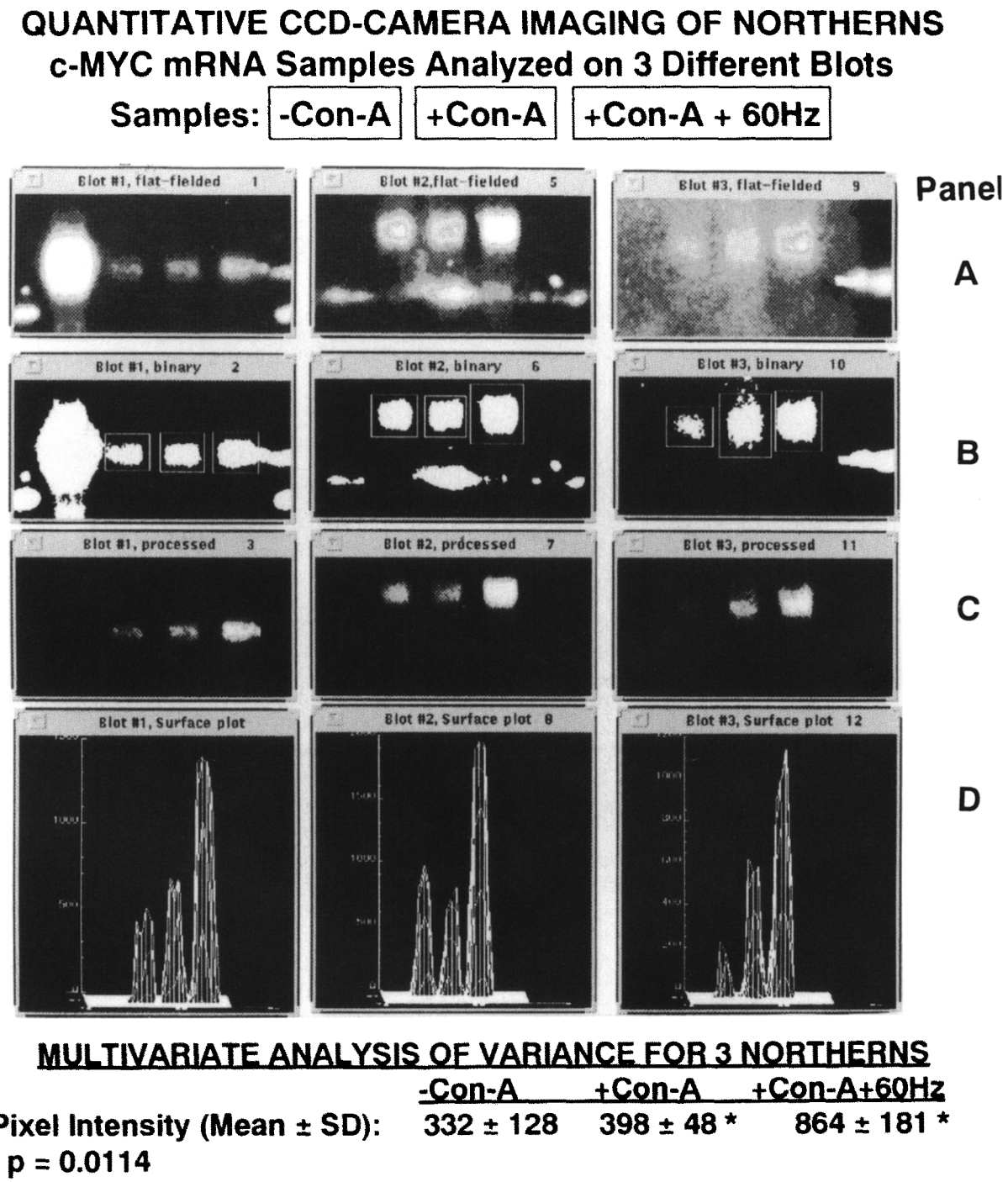

Fig. 3. Quantitative CCD-camera imaging of Northerns: comparison of three independent blots of the same RNA sample from one experiment. Each image contains three samples (left to right): −Con-A, +Con-A, and + Con-A plus magnetic field. Panels A show flat-fielded images of cMYC bands. Panels B show regions of interest for the bands. Panels C are thresholded images of the Northern blots. Panels D are surface plots of pixel intensity for bands in each image. Mean pixel intensities (arbitrary units) across three Northerns of the same sample: 332 ± 128 (−Con-A), 398 ± 48 (+Con-A), 864 ± 181 (MF + Con-A). Magnetic field exposure led to an approximate 2-fold increase in pixel intensity (P=0.011). Refer to Fig. 5 for conversion of these mRNA bands to relative hybridization ratios for c-MYC/GAPDH and comparison across three independent experiments.

thresholding. Panel D shows surface plots of pixel intensity for the bands in panels C. We compared the mean pixel intensity for these bands using a multivariate analysis of variance statistical program that analyzed for differences across bands in these experiments. Mean pixel intensity (arbitrary units ± S.D.) was −Con-A = 332 ± 128; +Con-A = 398 ± 48; +Con-A plus 60 Hz magnetic fields = 864 ± 181. A statistically significant difference was not detected between −Con-A and +Con-A ($P > 0.05$). A statistically significant difference was detected between +Con-A and +Con-A plus 60 Hz at the $P = 0.0114$ level (F ratio 16.71). Thus, it was

possible to obtain statistically significant results in the absence of O.D. calibration and GAPDH normalization.

In order to determine whether the above effect is specific for the c-MYC mRNA species or due to a general increase in mRNA abundance, we analyzed levels of RNA encoding a second 'housekeeping' protein, GAPDH, on the same blot. RNA samples from the above experiment, plus RNA samples from two additional, independent experiments were analyzed. For each Northern blot this standardization procedure involved normalizing the quantitated band intensity (O.D. × mm^2) for c-MYC by the associated band intensity for GAPDH. We provide evidence that GAPDH mRNA did not significantly vary across experimental treatment groups as shown in Fig. 4. A typical GAPDH

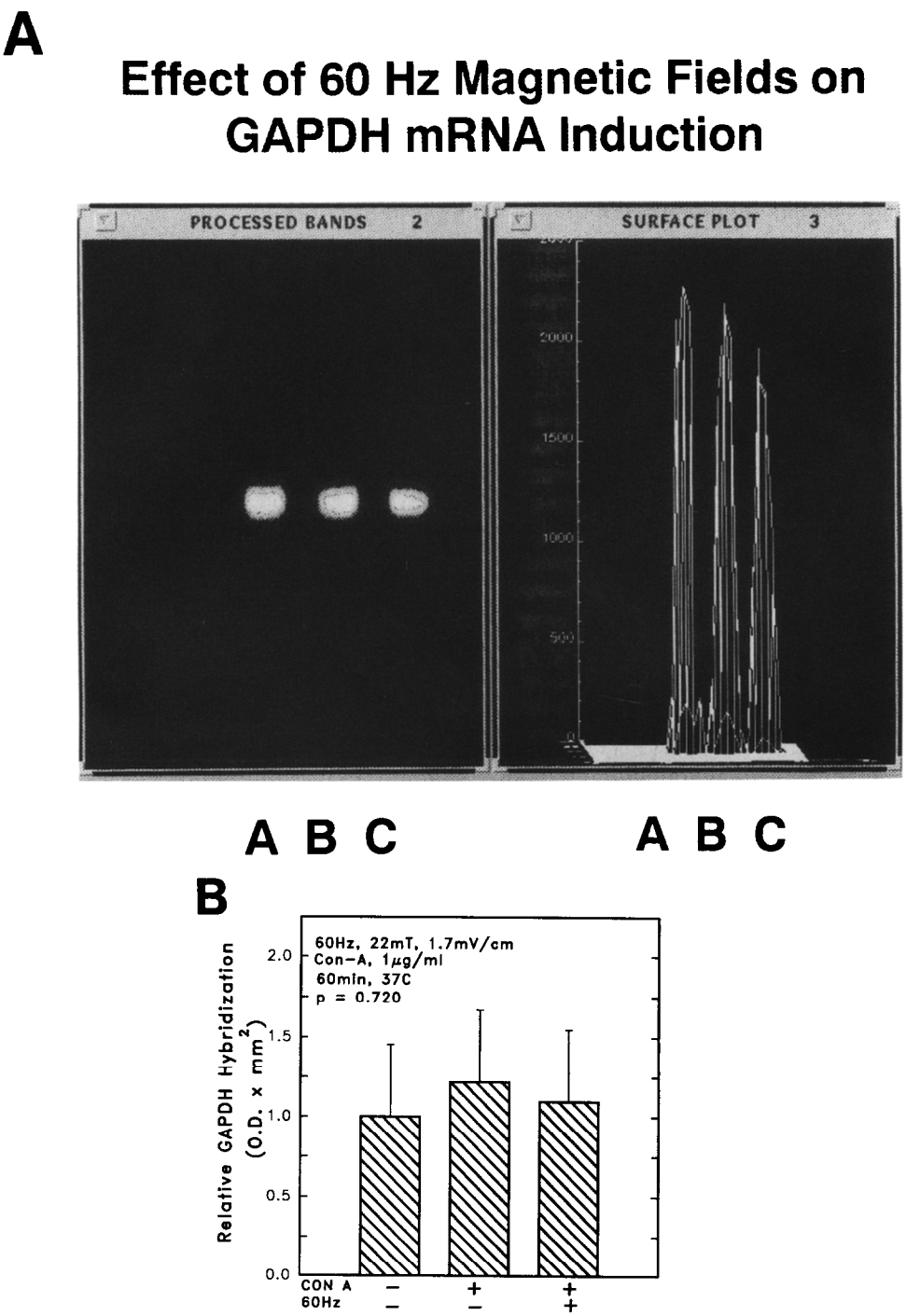

Fig. 4. 60 Hz magnetic fields do not influence GAPDH mRNA. (A) Quantitative CCD-camera imaging of northerns as described in Fig. 3. Treatment groups A, B, and C correspond to −Con-A, +Con-A, and +Con-A plus 60 Hz magnetic fields, respectively (see Figs. 2 and 3). (B) Composite data for GAPDH hybridization across three experiments in which calcium influx (Fig. 2) and c-MYC mRNA (Fig. 5) were also analyzed; mean ± S.D.

hybridization for one experiment is depicted in Fig. 4a with A, B, and C corresponding to −Con-A, +Con-A, and +Con-A plus 60 Hz treatments, respectively, as in Figs. 2 and 3. Bands were processed as described above and the right panel shows surface plots of pixel intensity for the bands with no evidence of major change across treatment groups. Composite GAPDH hybridization data across three experiments for these treatment groups is shown in Fig. 4b; GAPDH mRNA hybridization was set to one for un-stimulated cells (−Con-A) for comparison across experiments. GAPDH mRNA was not observed to be significantly influenced by 60 Hz magnetic fields.

Using GAPDH as a normalization parameter the relative ratios of c-MYC mRNA abundance to GAPDH abundance across experiments were computed; c-MYC/GAPDH ratio for non-activated (−Con-A) cells was set to one. Fig. 5 shows the ratio of c-MYC mRNA/GAPDH mRNA for cells in the three experiments of Figs. 2 and 4. Levels of c-MYC mRNA expression in non-activated cells were not statistically different than cells treated with a suboptimal dose of 1 μg/ml Con-A. In contrast, cells treated with Con-A plus magnetic fields exhibited an approximate 3.0-fold increase in c-MYC mRNA transcript levels that was statistically significant ($P < 0.026$, F ratio = 6.42). This pattern is consistent with the calcium influx data of Fig. 2.

3.3. *Evidence that calcium influx and c-MYC mRNA responses to magnetic fields are linked*

To provide additional support for linkage between c-MYC mRNA induction by magnetic fields and a magnetic field increase in calcium influx a further experiment was performed. We observed that thymocytes harvested from one group of litter mates failed to exhibit an increase in calcium influx in response to magnetic field exposure at 1 μg/ml Con-A, as used above. All three treatment groups, −Con-A, +Con-A, and +Con-A plus the magnetic field, exhibited identical calcium uptake. Although we do not know why this response was observed, we hypothesize that the Con-A dose employed was far from the threshold region for suboptimal Con-A activation; typically a sigmoidal curve is observed as Con-A concentration is increased with the suboptimal dose defined as that associated with the upward bend or 'knee' of the curve. If the 1 μg/ml dose was far removed from this suboptimal region then the magnetic field could not act as a co-stimulus and activation would not be detected. As mentioned above, other factors that influence Con-A responsiveness are animal age, concentration of mitogen, and immune status of the animal.

Analysis of RNA samples from this experiment revealed that the level of c-MYC mRNA transcripts were similar across treatment groups (data not shown). This indicates that the magnetic field failed to elevate c-MYC mRNA levels in cells that also failed to exhibit an increase in calcium influx. This negative finding plus the positive findings presented above (Figs. 2 and 5) strongly suggest the calcium and c-MYC mRNA responses to the magnetic field are linked. This correlation is consistent with a magnetic field interaction involving alterations in calcium influx and c-MYC transcription mediated via the signal transduction pathway.

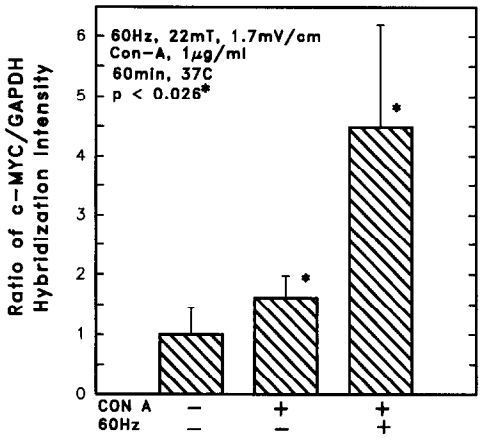

Fig. 5. 60 Hz magnetic fields increase c-MYC mRNA transcript levels. Relative transcript levels for c-MYC mRNA were standardized to the housekeeping enzyme GAPDH using quantitation by cooled-CCD image analysis. Composite data across three experiments in which calcium influx (Fig. 2) and GAPDH mRNA (Fig. 4) were also analyzed; mean ± S.E.

4. DISCUSSION

In this study we have assessed two early signal transduction markers, calcium ion influx and c-MYC mRNA expression, for the first time in the *same* cell population exposed to 60 Hz magnetic fields. A special annular cylindrical glass vessel was designed to test the hypothesis that magnetic field-induced increases in calcium influx are linked to mRNA induction via the ST cascade. The results presented here provide experimental evidence for such a linkage. This linkage is important since it supports a general biological framework for understanding how magnetic fields interact with cells and underscores the important role that signal transduction can play in magnetic field interactions with cellular systems.

The present study builds on previous reports that 60 Hz magnetic fields identical to those used here act to increase calcium ion influx in thymic lymphocytes during mitogen activation (22 mT; maximum $E_{induced}$ = 1.7 mV/cm) [1]. These studies also presented the first real time measurements of $[Ca^{2+}]_i$ during field exposure using a specially designed fluorescence exposure cuvette. These measurements identified the movement of extracellular calcium across the cell membrane into the cell as being responsible for the magnetic field elevation of $[Ca^{2+}]_i$, in contrast to the release of calcium from intracellular stores. This field response is dependent on

animal age and the state of the animal's immune system [11,18], and, importantly, is dependent on the induced electric field generated by the applied magnetic field according to Faraday's Law [1]. The latter is of mechanistic importance since the outer cell surface experiences an induced electric field proportional to the radius of the annular glass vessel (maximum radius = 4.0 cm), as compared to the induced electric field experienced by intracellular structures in the cell (maximum radius = ~ 4.0 μm). This represents a difference in magnitude of at least 10^4. In contrast to single cells in suspension, however, it is possible for adherent cells to maintain electrical contact with neighboring cells via tight junctions and, in this case, a rather large electrically conductive loop may be formed in a large array of cells [30,31]. Such systems are expected to exhibit lower thresholds for a field response.

How do ELF magnetic fields interact with cells to alter DNA and RNA synthesis? This question was first raised by reports of magnetic field effects on RNA, DNA, and protein synthesis [19–22]. These studies plus previous studies in which magnetic fields were shown to alter calcium influx [1,6,11,18], when taken together, suggest a role for ST in cell responses to magnetic fields. The ST interaction paradigm fits available experimental evidence and is consistent with biological mechanisms in cell signaling that regulate cell growth and differentiation. The findings we present here add further support to this paradigm by providing experimental evidence for a link between calcium influx and mRNA induction in magnetic fields via the ST cascade. Although the precise molecular event(s) involved in the field interaction are not yet known, the ST hypothesis requires that a cell surface/membrane interaction occurs which triggers the ST cascade and propagates the signal. The sequelae in the ST pathway for lymphocytes are shown in Table I and after Con-A binding to the T-cell receptor at the cell surface, a series of events occur including very early influx of extracellular calcium through a specialized ligand-gated channel. Following a rise in intracellular calcium and pH [32,33], detectable within minutes, the strong induction of c-MYC mRNA occurs within the first hour of the G1 phase [34]. In our studies calcium ion influx plays the role of triggering the ST cascade during magnetic field exposures. That this interaction is restricted to propagating down the ST cascade is strongly supported by our observation that magnetic field exposures failed to induce GAPDH (Fig. 4), a general housekeeping gene, but did induce c-MYC which is specifically involved in cell signaling.

Table I

Mitogen-activated signal transduction in the T-lymphocyte

RESPONSE TO CONCANAVALIN A	FIRST DETECTED
$[Ca+2]_i$, Calcium influx $[pH]_i$ IP_3 Increase PKC Activation	0 - 5 Minutes
c-FOS mRNA Increase c-MYC mRNA Increase Stimulation of Glycolysis Increase Metabolite Uptake (e.g. Uridine) Increased Inositol Incorporation into IPs	5 - 50 Minutes
Increased General Protein Synthesis Increased General RNA Synthesis Increased General DNA Synthesis	> 300 Minutes

Recently time-varying magnetic fields were reported to increase protein kinase C (PKC) activation in human leukemic HL-60 cells; importantly, PKC activation was diminished during field exposures by chelating extracellular calcium with EGTA [35]. Since calcium influx leads to PKC activation these findings lend additional support for an ST interaction in which calcium ions initiate effects of magnetic fields via the ST cascade.

The ST cascade depicted in Table I will ultimately lead to mitogenesis and cell proliferation. Such changes in cell status are profound and it is of interest that in the studies reported here magnetic fields were able to trigger two, linked, ST events at suboptimal doses of mitogen. This indicates that magnetic fields can act as co-stimulus when mitogen itself has a negligible effect on ST. Such a synergistic action with low doses of mitogenic inducers will have pronounced physiological changes for the cell. For example, in vivo evidence for a synergistic interaction between magnetic fields and a tumor promoter on the rate of tumor cell development was reported in a recent animal study [36]. These studies demonstrated that magnetic fields acted as a co-promoter in combination with *suboptimal* levels of 12-*O*-tetradecanoylphorbol-13-acetate (TPA) during magnetic field exposures of mice initiated with 7–12-dimethylbenzanthracene (DMBA) to produce papillomas. These results plus our in vitro findings support the idea that magnetic fields have the ability to act as a co-stimulus that potentiates cell signaling.

The general mechanism of the ST cascade amplifying a cell membrane-level magnetic field effect on a second messenger has application to a wide number of cell interactions. A variety of membrane-dependent events such as antibody-antigen binding followed by lymphocyte activation, and hormone binding with subsequent biochemical responses fit this paradigm. The salient features are that a cell membrane event is altered by the induced electric field acting at the cell surface, and this alteration is propagated via biochemical pathways to the cell interior where it is amplified. It is anticipated that specific examples other than T-cell activation will ultimately emerge from future studies of ELF magnetic fields and cellular systems. For example, evidence was recently reported that 1.2 μT (12 mG) 60 Hz magnetic fields block melatonin's oncostatic action on the proliferation of MCF-7 cells, a human breast cancer cell line [37]. In this model system melatonin is thought to bind to a receptor, possibly the estrogen receptor, and subse-

quently down regulate MCF-7 proliferation. Magnetic fields of 1.2 μT (12 mG), but not 0.2 μT (2 mG) were observed to completely block this growth inhibition.

Further mechanistic studies in such systems and in the T-cell system discussed above are required in order to understand specific molecular events that occur in the cell during field exposure. For example, it would be desirable to identify the first site of interaction in the ST cascade influenced by magnetic fields. Con-A binding to the T-cell receptor is the first event in ligand-mediated T-cell activation, and up or down regulation of calcium influx may be directly mediated by alterations in Con-A binding. A relevant question is whether Con-A binding is directly altered by magnetic fields, and we are approaching this question at the single-cell level using quantitative fluorescence photometry and cooled-CCD digital imaging fluorescence microscopy. Alternatively, immediately following Con-A binding, tyrosine kinase activity is triggered within the first few seconds of TCR ligation and this is thought to initiate the $[Ca^{2+}]_i$ signal [38]; this activity may be influenced by magnetic fields. Studies such as these that asses the ST cascade in a wide variety of cell systems will help to identify common modes of magnetic field interactions with cells. In addition, in the studies presented here, characterization of parameters such as the dose-dependence for field intensity, length of exposure, reversibility for the effect, and the influence of calcium channel blockers need to be investigated.

Acknowledgements: Support for this research was provided in part by the Office of Energy Management, Utilities Systems Division, the Office of Health and Environmental Research, U.S. Department of Energy under Contract DE-AC03-76SF00098, and the NIH under Grant CA53711(RPL) from the NCI.

REFERENCES

[1] Liburdy, R.P. (1992) FEBS Lett. 301, 53–59.
[2] Adey, W.R. (1988) Neurochem. Res. 13, 671–677.
[3] Luben, R.A (1991) Health Phys. 61, 15–28.
[4] Chiabrera, A., Nicolini, C. and Schwan, H.P. (Eds.) (1985) Interactions Between Electromagnetic Fields and Cells, Plenum, New York.
[5] Tenforde, T.S. (1992) Annu. Rev. Public Health 13, 173–196.
[6] Walleczek, J. and Liburdy, R.P. (1990) FEBS Lett. 271, 157–160.
[7] Yost, M.G. and Liburdy, R.P.(1992) FEBS Lett. 296, 117–122.
[8] Lyle, D.B., Ayotte, R.D., Sheppard, A.R., and Adey, W.R. (1988) Bioelectromagnetics 9, 303–313.
[9] Lyle, D.B. Xinghua, W., Ayotte, R.D., Sheppard, A.R. and Adey, W.R. (1991) Bioelectromagnetics 12, 145–156.
[10] Carson, J.J.L., Prato, F.S., Drost, D.J., Diesbourg, L.D. and Dixon, S.J. (1990) Am. J. Physiol. 259, C687–692.
[11] Liburdy, R.P. (1992) Ann. N.Y. Acad. Sci. 649, 74–95.
[12] Blackman, C.F., Benane, S.G., Rabinowitz, J.R., House, D.E. and Joines, W.T. (1985) Bioelectromagnetics 6, 327–337.
[13] Blackman, C.F., Benane, S.G., Elliot, D.J., House, D.E. and Pollock, M.M. (1988) Bioelectromagnetics 9, 215–227.
[14] Blackman, C.F., Benane, D.J., House, D.E. and Elliot, D.J. (1990) Bioelectromagnetics 11, 159–167.
[15] Bawin, S.M. and Adey, W.R. (1976) Proc. Natl. Acad. Sci. USA 73, 1999–2003.
[16] Gardner, P. (1989) Cell 59, 15–20.
[17] Berridge, M.J. and Irvine, R.F. (1989) Nature 341, 197–205.
[18] Liburdy, R.P. (1992) in: Interaction Mechanisms of Low-Level Electromagnetic Fields in Living Systems (Norden, B. and Ramel, C., Eds.) pp. 217–239, Oxford University Press, New York.
[19] Goodman, R., Wei, L.-X., Xu, J.-C. and Henderson, A.S. (1989) Biochim. Biophysic. Acta 1009, 216–220.
[20] Goodman, R. and Henderson, A.S. (1991) Bioelectrochem. Bioenerg. 25, 335–355.
[21] Goodman R., Bumann, J., Wei, L.-X., Shirley-Henderson, A. (1992) Electro. Magnetobiol. 11(1), 19–28.
[22] Phillips, J.L., Haggren, W., Thomas, W.J., Ishida-Jones, T. and Adey, W.R. (1992) Biochim. Biophys. Acta 1132, 140–144.
[23] Liburdy, R.P., Callahan, D.E., Sloma, T.R., Yaswen, P. (1992) First World Congress for Electricity and Magnetism in Biology and Medicine, June 14–19, Lake Buena Vista, FL, USA. Abstract B-10.
[24] Tenforde T.S. and Kaune, W.T. (1987) Health Phys. 53, 585–606.
[25] Bassen, H., Litovitz, T., Penafiel, M. and Meister, R. (1992) Bioelectromagnetics 13, 183–198.
[26] Yaswen, P., Smoll, A., Peehl, D., Trask, D., Sager, R. and Stampfer, M. (1990) Proc. Natl. Acad. Sci. USA 87, 7360–7364.
[27] Stanton, L., Watt, R. and Marcu, K. (1983) Nature 303, 401–402.
[28] Takahama, Y., Shores, E.W. and Singer, A. (1992) Science 258, 653–656.
[29] Correa-Rotter, R., Mariash, C.N. and Rosenberg, M.E. (1992) Biotechniques 12, 154–158.
[30] Polk, C. (1992) Bioelectromagnetics Suppl. 1, 209–235.
[31] Pilla,A.A., Nasser, P.R. and Kaufman, J.J. (1992) First World Congress for Electricity and Magnetism in Biology and Medicine, June 14–19, Lake Buena Vista, FL, USA. Abstract P-66.
[32] Grinstein, S., Smith, J., Onizuka, R., Cheung, R. and Gelfand, E. (1988) J. Biol. Chem. 263, 8658–8665.
[33] Dixon, S.J., Stewart, D., Grinstein, S. and Spiegel, S. (1987) J. Cell Biol. 105, 1153–1161.
[34] Marcu, K., Bossone, S.A. and Patel, A.J. (1992) Annu. Rev. Biochem. 61, 809–860.
[35] Monti, M.G., Pernecco, L., Moruzzi, M.S., Battini, R., Zanoli, P. and Barbiroli, B. (1991) J. Bioelectr. 10, 119–130.
[36] Stuchly, M.A., McLean, J.R.N., Burnett, R., Goddard, M., Lecuyer, D. and Mitchell, R.E.J. (1992) Cancer Lett. 65, 1–7.
[37] Liburdy, R.P., Sloma, T.R., Sokolic, R. and P. Yaswen (1993) J. Pineal Res. 14, 89–97.
[38] Wolff, C.H.J., Hong, S.-C., von Grafenstein, H. and Janeway, C.A. (1993) J. Immunol. 151, 11337–1345.